Available online at www.sciencedirect.com
SCIENCE DIRECT®
International Journal of Thermal Sciences 42 (2003) 1145–1152
International Journal of Thermal Sciences
www.elsevier.com/locate/ijts

Melting of PCM around a horizontal cylinder with constant surface temperature

Kamal A.R. Ismail, Maria das Graças E. da Silva

Department of Thermal and Fluid Engineering, Faculty of Mechanical Engineering, State University of Campinas, 13083, Campinas, SP, Brazil

Received 27 May 2002; accepted 21 March 2003

Abstract

A numerical study of melting of phase change material (PCM) around a horizontal circular cylinder of constant wall temperature and in the presence of the natural convection in the melt region is presented. A two dimensional mathematical model is formulated in terms of primitive variables and a coordinate transformation technique is used to fix the moving front. The finite volume approach is used to discretize the system of governing equations to obtain a system of linear algebraic equations. An implicit scheme is used for the momentum and energy equations and an explicit scheme for the energy balance at the interface. The numerical predictions were compared with available results to establish the validity of the model and additional results are obtained to demonstrate the effects of Rayleigh and Stefan numbers as well as the wall temperature on the time for complete fusion and total melt volume.

Keywords: Fusion of PCM; Phase change; Horizontal cylinder

1. Introduction

Problem of heat transfer with phase change is extremely important in latent heat storage systems and many other thermal applications. The literature is very rich with studies of heat transfer with phase change based upon pure conduction formulation. The presence of natural convection in the melt region during fusion may lead to increasing the heat transfer rate and causes the predictions based upon pure conduction to be non-realistic.

Basically there are two methods for formulating the problem of heat transfer with phase change. The first method uses the temperature as a dependent variable while the second uses the enthalpy as a dependent variable in the energy equation. In the models based upon the temperature, the energy equation is written separately for each phase and the coupling between the two equations is done through the energy balance at the solid–liquid interface. In this type of formulation it is necessary to know explicitly the position of the interface in order to determine the temperature. Having a moving interface not known before hand complicates the problem and its solution. One of the methods to solve the problem is to immobilize the interface as done by Landau [1], Duda et al. [2], Saitoh [3] and Sparrow et al. [4]. A second method is to use the enthalpy as a dependent variable and hence can write a single energy equation for the whole domain, liquid and solid. This method has the advantage of not requiring to determine the interface position in order to solve the energy equation. Comparative studies of the two methods can be found in Furzerland [5] and Viswanath and Jaluria [6]. A pioneer study realized by Sparrow et al. [7] of fusion around a vertical cylinder showed that natural convection could not be ignored in the analysis of fusion problems. Later Yao and Chen [8] determined an approximate solution for the fusion problem around a horizontal constant temperature cylinder by using the perturbation technique. They studied the effect of natural convection on the fusion process and concluded that it depends strongly on the Rayleigh number. Yao and Cherney [9] solved the case of fusion around a horizontal constant temperature cylinder by using the integral method. Rieger et al. [10] solved numerically the problem of fusion around a horizontal cylinder under the conditions of constant wall temperature and constant heat flux over the cylinder wall. They included natural convection in the liquid phase and used body fitted coordinate technique to immobilize the fusion front. Prusa and Yao [11,12] analysed numerically the effects of natural convection during the process of fusion around a horizontal cylinder. They used the technique of co-

E-mail address: kamal@fem.unicamp.br (K.A.R. Ismail).

1290-0729/$ – see front matter
doi:10.1016/S1290-0729(03)00093-0

Nomenclature

c_p	specific heat	$J\cdot kg^{-1}\cdot K^{-1}$	
Fo	Fourier number, $=\alpha t/r_o^2$		
g	gravity acceleration	$m\cdot s^{-2}$	
k	thermal conductivity	$W\cdot m^{-1}\cdot K^{-1}$	
L	latent heat	$J\cdot kg^{-1}$	
P	dimensionless pressure		
Pr	Prandtl number, $=\nu/\alpha$		
r_o	cylinder radius	m	
r	radial coordinate	m	
r_L	interface position	m	
R	dimensionless radial coordinate, $=r/r_o$		
R_L	dimensional interface position, $=r_L/r_o$		
Ra	Rayleigh number, $=g\beta(T_o-T_m)r_o^3/\nu\alpha$		
Ste	Stefan number based on temperature, $=c_p(T_o-T_m)/L$		
t	time	s	
T	temperature of the liquid phase	K	
V_θ	dimensionless velocity component in the tangential direction		
V_R	dimensionless velocity component in the radial direction		

Greek symbols

α	thermal diffusivity	$m^2\cdot s^{-1}$
β	coefficient of thermal expansion	K^{-1}
ϕ	dimensionless temperature	
Δ_L	dimensionless melt thickness, $=R_L-1$	
η	transformed radial coordinate, $=\frac{r-r_o}{r_L-r_o}=\frac{R-1}{\Delta_L}$	
μ	dynamic viscosity	$kg\cdot m^{-1}\cdot s^{-1}$
ν	kinematic viscosity	$m^2\cdot s^{-1}$
θ	angular coordinate	
ρ	specific mass	$kg\cdot m^{-3}$
τ	dimensionless time, $=\frac{\alpha_L t}{r_o^2}\,Ste$	
τ_{tot}	complete fusion time	hour
$\bar{\Lambda}, \Lambda, \Theta, \Omega, \Psi$	auxiliary variables	
$\forall$	volume	

Superscript

$*$	dimensionless variables

Subscripts

L	liquid
m	phase change
o	surface of the cylinder
R	radial direction
tot	total
θ	angular direction

ordinate transformation to fix the irregular moving interface and finite difference approach to solve the problem numerically. Additional experimental results and comparisons were realized by Hermann et al. [13] and Ho and Chen [14].

The formulation of the problem of melting around a circular cylinder as available in Yao and Chen [8], Yao and Cherney [9], Rieger et al. [10] and Prusa and Yao [11, 12] is formulated based upon the stream function and vorticity method, while the work of Sparrow et al. [7] is based upon primitive variables formulation. In Sparrow et al. [7] work, the terms resulting from the transformation of coordinates were eliminated in order to simplify the numerical solution of the problem and hence their solution is approximate. The contribution of the present study to the actual knowledge lies in the fact that the problem is formulated using primitive variables. The equations were treated by using a transformation of coordinates which leads to immobilize the moving front. The resulting system of equations, including complicated terms resulting from the coordinate transformation process were treated numerically by using the control volume approach. The proposed model and numerical code are part of a detailed study to provide some numerical codes to handle different practical problems of interest in energy storage modelling and analysis.

This paper deals with the numerical study of melting of phase change material (PCM) around a horizontal circular cylinder in the presence of natural convection in the melt phase. A two dimensional non-steady mathematical model has been formulated in terms of the primitive variables and a coordinate transformation has been used to fix the moving interface. The finite volume approach was used to discretize the system of governing equations and the associated boundary and initial conditions to obtain a system of linear algebraic equations. The numerical code was optimized and the numerical predictions were compared with available numerical results to establish the validity of the model and the numerical approach.

2. Mathematical model

The physical problem is shown in Fig. 1. The horizontal cylinder of radius r_o is immersed in an infinite solid PCM. At the instant $t=0$, the PCM is at the phase change temperature T_m. When the cylinder surface temperature is at $T_o > T_m$, the fusion process starts. Two fusion cases will be treated here. The first, when the surface temperature of the cylinder $T_o > T_m$ while the other of specified heat flux q. The general simplifications considered in this study include transient formulation and two dimensional Newtonian incompressible fluid where the natural convection effects are considered. The thermophysical properties of the PCM are assumed constant except the density.

The basic equations can be written as:

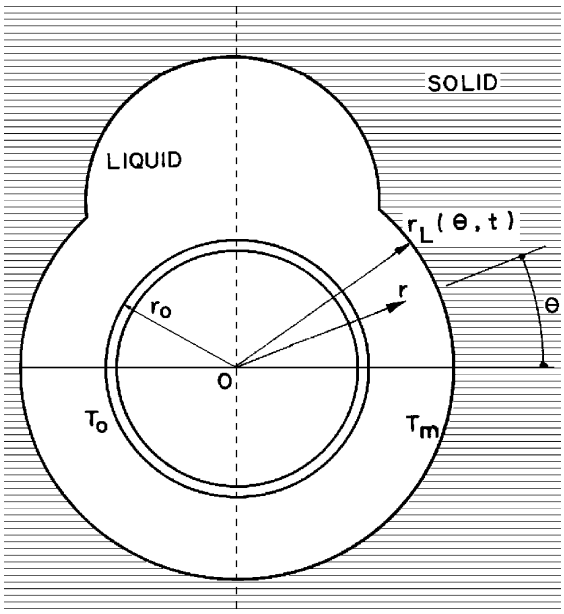

Fig. 1. Layout of the physical problem.

Energy conservation equation

$$\frac{\partial T}{\partial t}+\frac{1}{r}\frac{\partial(rV_R^*T)}{\partial r}+\frac{1}{r}\frac{\partial(V_\theta^*T)}{\partial\theta} =\alpha\left(\frac{1}{r}\frac{\partial}{\partial r}\left(r\frac{\partial T}{\partial r}\right)+\frac{1}{r^2}\frac{\partial^2 T}{\partial\theta^2}\right) \tag{1}$$

Mass conservation equation

$$\frac{1}{r}\frac{\partial(rV_R^*)}{\partial r}+\frac{1}{r}\frac{\partial V_\theta^*}{\partial\theta}=0 \tag{2}$$

Equation of motion in the tangential direction

$$\frac{\partial V_\theta^*}{\partial t}+\frac{1}{r}\frac{\partial(rV_R^*V_\theta^*)}{\partial r}+\frac{1}{r}\frac{\partial(V_\theta^*)^2}{\partial\theta}+\frac{V_R^*V_\theta^*}{r} =-\frac{1}{\rho}\frac{1}{r}\frac{\partial P^*}{\partial\theta}+\bar{\Lambda}\cos\theta +\nu\left(\frac{1}{r}\frac{\partial}{\partial r}\left(r\frac{\partial V_\theta^*}{\partial r}\right)+\frac{1}{r^2}\frac{\partial^2 V_\theta^*}{\partial\theta^2}-\frac{V_\theta^*}{r^2}+\frac{2}{r^2}\frac{\partial V_R^*}{\partial\theta}\right) \tag{3}$$

Equation of motion in the radial direction

$$\frac{\partial V_R^*}{\partial t}+\frac{1}{r}\frac{\partial r(V_R^*)^2}{\partial r}+\frac{1}{r}\frac{\partial(V_\theta^*V_R^*)}{\partial\theta}-\frac{(V_\theta^*)^2}{r} =-\frac{1}{\rho}\frac{\partial P^*}{\partial r}+\bar{\Lambda}\sin\theta +\nu\left(\frac{1}{r}\frac{\partial}{\partial r}\left(r\frac{\partial V_R^*}{\partial r}\right)+\frac{1}{r^2}\frac{\partial^2 V_R^*}{\partial\theta^2}-\frac{V_R^*}{r^2}-\frac{2}{r^2}\frac{\partial V_\theta^*}{\partial\theta}\right) \tag{4}$$

where the term $\bar{\Lambda}$ is given by $\bar{\Lambda}=\beta g(T-T_m)$

The initial and boundary conditions for Eqs. (1)–(4) are

$$T=T_m,\qquad V_\theta^*=0,\qquad V_R^*=0\quad \text{at } t=0 \tag{5}$$

$$T=T_o,\qquad V_\theta^*=0,\qquad V_R^*=0\quad \text{at } r=r_o,\ t>0 \tag{6}$$

$$\frac{\partial T}{\partial\theta}=0,\qquad V_\theta^*=0,\qquad \frac{\partial V_R^*}{\partial\theta}=0 \quad \text{at } \theta=\pm\frac{\pi}{2},\ t>0 \tag{7}$$

The boundary conditions at the solid–liquid interface are given by

$$T=T_m,\qquad V_\theta^*=0,\qquad V_R^*=0\quad \text{at } r=r_L,\ t>0 \tag{8}$$

$$\left[1+\left(\frac{1}{r_L}\frac{\partial r_L}{\partial\theta}\right)^2\right]\left(-k\frac{\partial T}{\partial r}\right)=\rho L\frac{\partial r_L}{\partial t} \quad \text{at } r=r_L,\ t>0 \tag{9}$$

The problem of phase change in the presence of natural convection is extremely difficult to handle. To reduce these difficulties, the front immobilisation technique is used where the coordinates r and θ are transformed to η and θ where

$$\eta=\frac{r-r_o}{r_L-r_o}$$

And the new domain is defined by $0\leqslant\eta\leqslant 1$ and $-\pi/2\leqslant\theta\leqslant\pi/2$.

In order to facilitate the numerical calculations the new coordinate system and also new dimensionless variables are adopted. These variables are

$$R=\frac{r}{r_o}\quad\text{and}\quad R_L=\frac{r_L}{r_o}$$

$$\Delta_L=R_L-1\quad\text{and}\quad\eta=\frac{R-1}{\Delta_L}$$

$$\tau=\frac{\alpha_L t}{r_o^2}\,Ste,\qquad\phi=\frac{T-T_m}{T_o-T_m}$$

$$V_\theta=\frac{V_\theta^* r_o}{\alpha},\qquad V_R=\frac{V_R^* r_o}{\alpha}$$

$$P=\frac{P^*}{\rho(\alpha/r_o)^2},\qquad Ste=\frac{c_p(T_o-T_m)}{L}$$

Substituting the new variables in Eqs. (1)–(9), these equations are written as below.

Equation of energy conservation

$$Ste\frac{\partial\phi}{\partial\tau}+\frac{1}{R\Delta_L}\frac{\partial}{\partial\eta}(RV_R\phi)+\frac{1}{R}\frac{\partial(V_\theta\phi)}{\partial\theta} =\frac{1}{R\Delta_L}\frac{\partial}{\partial\eta}\left(\frac{R}{\Delta_L}\frac{\partial\phi}{\partial\eta}\right)+\frac{1}{R^2}\frac{\partial^2\phi}{\partial\theta^2}+\Omega_{\text{liq}} \tag{10}$$

where

$$\Omega_{\text{liq}}=\frac{\eta\,Ste}{\Delta_L}\frac{\partial\Delta_L}{\partial\tau}\frac{\partial\phi}{\partial\eta}+\frac{\eta}{R\Delta_L}\frac{\partial\Delta_L}{\partial\theta}\frac{\partial(V_\theta\phi)}{\partial\eta} +\frac{2\eta}{R^2\Delta_L^2}\left(\frac{\partial\Delta_L}{\partial\theta}\right)^2\frac{\partial\phi}{\partial\eta}-\frac{\eta}{R^2\Delta_L}\frac{\partial^2\Delta_L}{\partial\theta^2}\frac{\partial\phi}{\partial\eta} -\frac{\eta}{R^2\Delta_L}\frac{\partial\Delta_L}{\partial\theta}\frac{\partial^2\phi}{\partial\theta\partial\eta}$$

Mass conservation equation

$$\frac{1}{R\Delta_L}\frac{\partial}{\partial\eta}(RV_R)+\frac{1}{R}\frac{\partial V_\theta}{\partial\theta}-\Omega_{\text{cm}}=0 \tag{11}$$

where

$$\Omega_{\rm cm} = \frac{\eta}{R\Delta_L}\frac{\partial \Delta_L}{\partial \theta}\frac{\partial V_\theta}{\partial \eta}$$

Equation of motion in the tangential direction

$$Ste\frac{\partial V_\theta}{\partial \tau} + \frac{1}{R\Delta_L}\frac{\partial}{\partial \eta}(RV_RV_\theta) + \frac{1}{R}\frac{\partial V_\theta^2}{\partial \theta} = -\frac{1}{R}\frac{\partial P}{\partial \theta} + \frac{1}{R\Delta_L}\frac{\partial}{\partial \eta}\left(\frac{Pr\,R}{\Delta_L}\frac{\partial V_\theta}{\partial \eta}\right) + \frac{Pr}{R^2}\frac{\partial^2 V_\theta}{\partial \theta^2} + \Psi_{\rm ang} + \Omega_{\rm ang} \quad (12)$$

where

$$\Psi_{\rm ang} = Pr\Lambda\cos\theta - \frac{V_\theta V_R}{R} - \frac{V_\theta Pr}{R^2} + \frac{2Pr}{R^2}\frac{\partial V_R}{\partial \theta}$$

and

$$\Omega_{\rm ang} = \frac{\eta}{R\Delta_L}\frac{\partial \Delta_L}{\partial \theta}\frac{\partial P}{\partial \eta} + \frac{\eta\,Ste}{\Delta_L}\frac{\partial \Delta_L}{\partial \tau}\frac{\partial V_\theta}{\partial \eta} + \frac{\eta}{R\Delta_L}\frac{\partial \Delta_L}{\partial \theta}\frac{\partial V_\theta^2}{\partial \eta} + \frac{2\eta Pr}{R^2\Delta_L^2}\left(\frac{\partial \Delta_L}{\partial \theta}\right)^2\frac{\partial V_\theta}{\partial \eta} - \frac{\eta Pr}{R^2\Delta_L}\frac{\partial^2 \Delta_L}{\partial \theta^2}\frac{\partial V_\theta}{\partial \eta} - \frac{\eta Pr}{R^2\Delta_L}\frac{\partial \Delta_L}{\partial \theta}\frac{\partial^2 V_\theta}{\partial \theta\,\partial \eta} - \frac{2\eta Pr}{R^2\Delta_L^2}\frac{\partial \Delta_L}{\partial \theta}\frac{\partial V_R}{\partial \eta}$$

Equation of motion in the radial direction

$$Ste\frac{\partial V_R}{\partial \tau} + \frac{1}{R\Delta_L}\frac{\partial}{\partial \eta}\left(RV_R^2\right) + \frac{1}{R}\frac{\partial (V_RV_\theta)}{\partial \theta} = -\frac{1}{\Delta_L}\frac{\partial P}{\partial \eta} + \frac{1}{R\Delta_L}\frac{\partial}{\partial \eta}\left(\frac{Pr\,R}{\Delta_L}\frac{\partial V_R}{\partial \eta}\right) + \frac{Pr}{R^2}\frac{\partial^2 V_R}{\partial \theta^2} + \Omega_{\rm rad} + \psi_{\rm rad} \quad (13)$$

where

$$\Psi_{\rm rad} = Pr\Lambda\sin\theta + \frac{V_\theta^2}{R} - \frac{V_RPr}{R^2} - \frac{2Pr}{R^2}\frac{\partial V_\theta}{\partial \theta}$$

and

$$\Omega_{\rm rad} = \frac{\eta}{R\Delta_L}\frac{\partial \Delta_L}{\partial \theta}\frac{\partial (V_\theta V_R)}{\partial \eta} + \frac{\eta Ste}{\Delta_L}\frac{\partial \Delta_L}{\partial \tau}\frac{\partial V_R}{\partial \eta} + \frac{2\eta Pr}{R^2\Delta_L^2}\left(\frac{\partial \Delta_L}{\partial \theta}\right)^2\frac{\partial V_R}{\partial \eta} - \frac{\eta Pr}{R^2\Delta_L}\frac{\partial^2 \Delta_L}{\partial \theta^2}\frac{\partial V_R}{\partial \eta} - \frac{\eta Pr}{R^2\Delta_L}\frac{\partial \Delta_L}{\partial \theta}\frac{\partial^2 V_R}{\partial \theta\,\partial \eta} + \frac{2\eta Pr}{R^2\Delta_L}\frac{\partial \Delta_L}{\partial \theta}\frac{\partial V_\theta}{\partial \eta}$$

The initial, boundary and interface conditions can be written as

$$\phi = 0, \qquad V_\theta = 0, \qquad V_R = 0 \quad \text{at } \tau = 0 \quad (14)$$

$$\phi = 1, \qquad V_\theta = 0, \qquad V_R = 0 \quad \text{at } \eta = 0,\ \tau > 0 \quad (15)$$

The interface conditions are

$$\phi = 0, \qquad V_\theta = 0, \qquad V_R = 0 \quad \text{at } \eta = 1,\ \tau > 0 \quad (16)$$

$$\left[1 + \left(\frac{1}{(\Delta_L + 1)}\frac{\partial \Delta_L}{\partial \theta}\right)^2\right]\left(-\frac{1}{\Delta_L}\frac{\partial \phi}{\partial \eta}\right) = \frac{\partial \Delta_L}{\partial \tau} \quad \text{at } \eta = 1,\ \tau > 0 \quad (17)$$

The finite volume approach was used to discretize the system of differential equations and obtain a system of linear algebraic equations. The numerical solution was determined using an implicit scheme for the momentum and energy equations and explicit scheme for the energy balance at the interface. Numerical tests were realized in order to optimise the computational grid. The number of grid points along the tangential direction is taken as 50 and 30 points along the radial direction.

3. Results and discussion

Rieger et al. [10] studied the problem of fusion around a horizontal cylinder under surface constant temperature. Their model is formulated based upon stream and vorticity functions and body fitted coordinates and finite difference approximation. Their results were compared with the numerical predictions from the present model. Figs. 2 and 3 show the thickness of the melt layer for values of $Ra = 10^4$ and $Ra = 37\,500$. As can be noticed the agreement is good. Figs. 4 and 5 show the variation of Nusselt number over the surface of the cylinder for the case of $Ra = 10^4$ and $Ra = 37\,500$. It is interesting to observe how the regimes of transition occur between dominant conduction and dominant convection as reported by Sparrow et al. [15]. During the dominant conduction process, the curves show a reduction in the Nusselt number. When the dominant convection regime is established the profiles seem to be constant. As

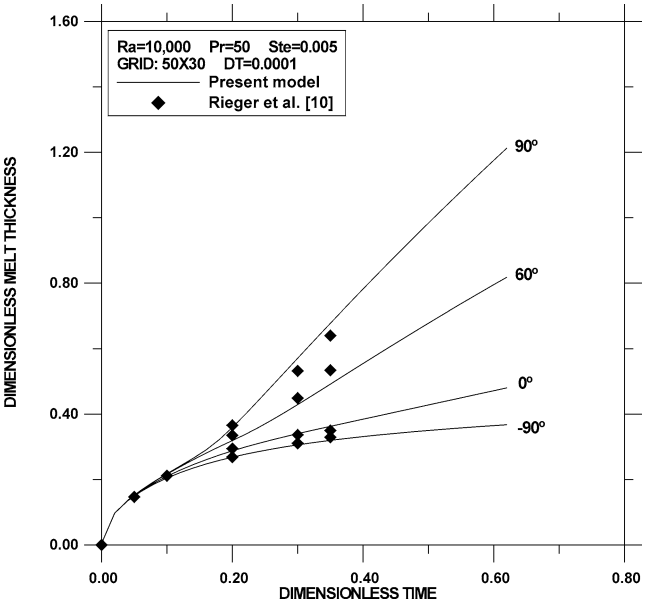

Fig. 2. Comparison of the predicted dimensionless melt thickness with the results of Rieger et al. [10].

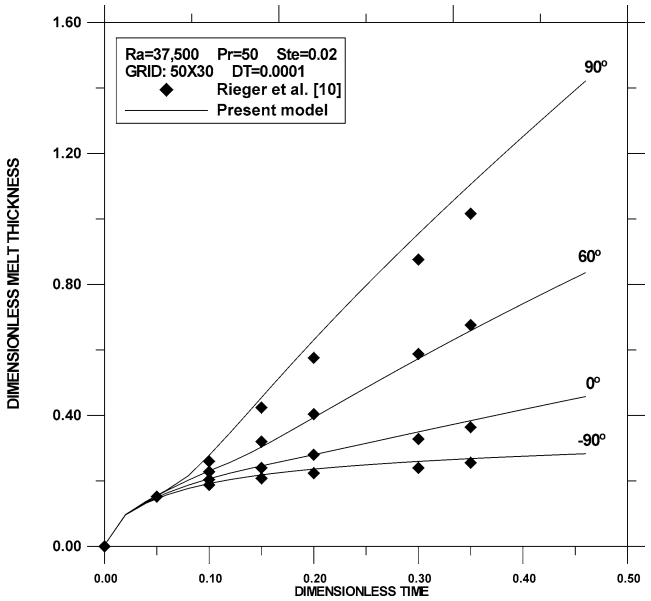

Fig. 3. Comparison of the predicted melt thickness with the results of Rieger et al. [10].

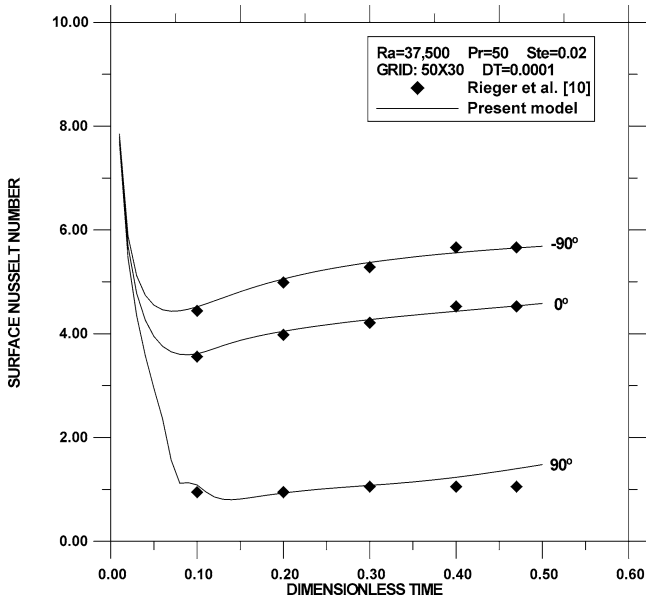

Fig. 5. Comparison of the predicted surface Nusselt number with the results of Rieger et al. [10] for $Ra = 37\,500$.

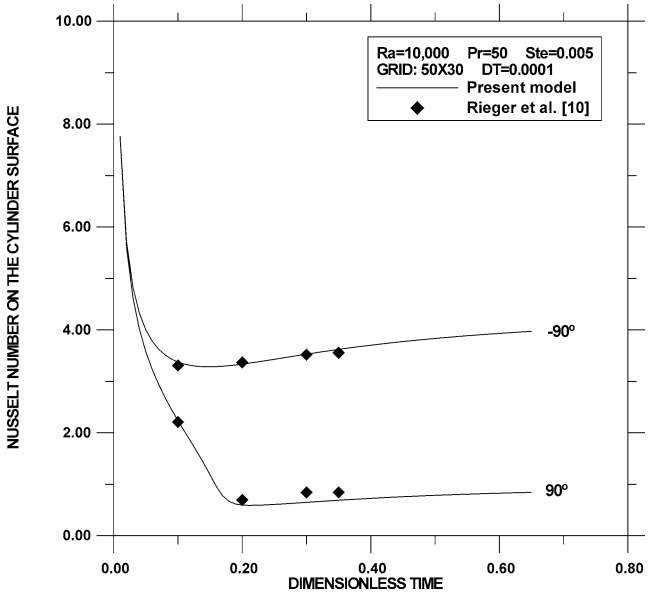

Fig. 4. Comparison of the predicted surface Nusselt number with the results of Rieger et al. [10] for $Ra = 10^4$.

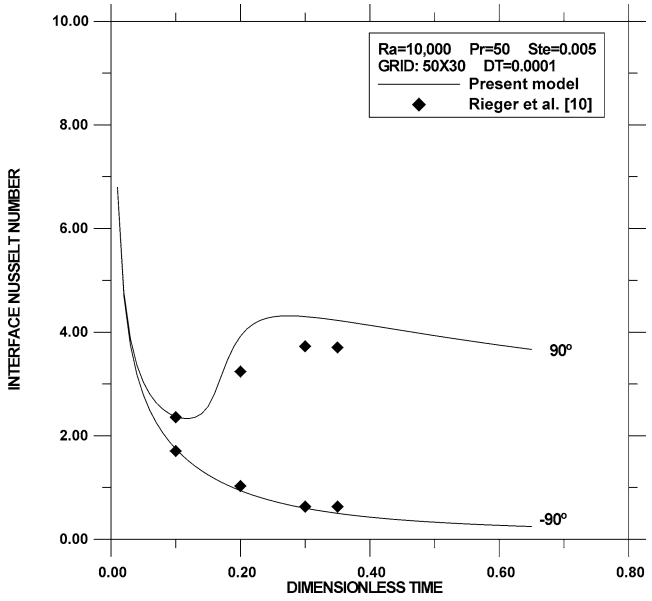

Fig. 6. Comparison of the predicted interface Nusselt number with the results of Rieger et al. [10] for $Ra = 10^4$.

can be seen the results agree well indicating that the present model is able to predict precise results. Figs. 6 and 7 show comparisons of Nusselt number at the liquid–solid interface as calculated by Rieger et al. and the present model. The results seem to agree very well for the case of $\theta = -90°$ but differs slightly for the position $\theta = 90°$ although keeping the same tendency. Figs. 8 and 9 show the melt volume as calculated by Rieger et al. and the present model for the two cases of $Ra = 10^4$ and $Ra = 37\,500$ showing good agreement between the results. Figs. 14 and 15 show that after convection been established, the variation of the melt volume with time seems to the linear as reported by Hale and Viskanta [16].

Additional results from the present model were obtained using n-octadecane as a PCM and a cylinder of external radius $r_o = 0.00476$ m. The n-octadecane was the most preferred because of its phase change temperature and also widely used and hence easy to find relevant literature. The thermal properties of this PCM based upon Bernard et al. [17] are shown in Table 1.

Fig. 10 shows the time for complete fusion in terms of the Rayleigh number. It is found that for Rayleigh number more than 24 000, the time for complete fusion seems to increase at a much lower rate than for cases of $Ra < 24\,000$. This can be attributed to the fact that the increase in Rayleigh number

Table 1
Thermal properties of liquid n-octadecane

Melting point [K]	ρ [kg/m^3]	k [W/m·K]	Cp [J/kg·K]	μ [kg/m·s]	ν [m^2/s]	L [J/kg]	β [1/K]	Pr
301.2	776.8	0.157	2200	3.878×10^{-3}	5.005×10^{-6}	241000	9.1×10^{-4}	54.5

Source: Benard et al. [17].

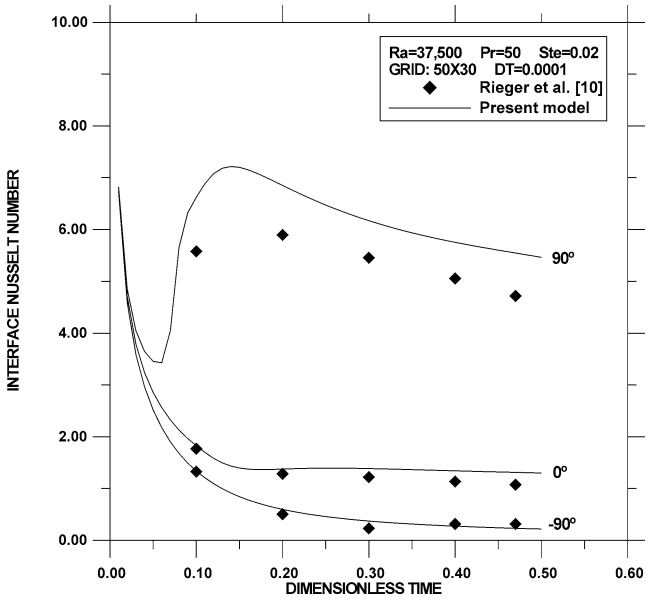

Fig. 7. Comparison of the predicted interface Nusselt number with the results of Rieger et al. [10] for $Ra = 37\,500$.

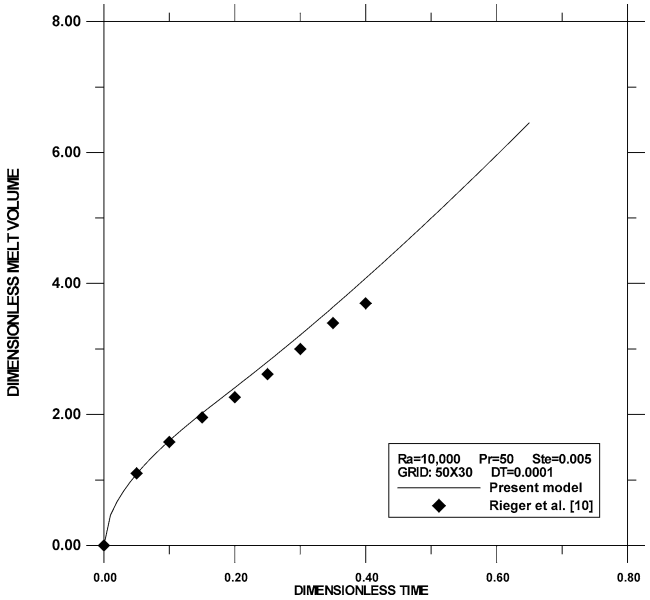

Fig. 8. Comparison of the predicted dimensionless melt volume with the results of Rieger et al. [10] for $Ra = 10^4$.

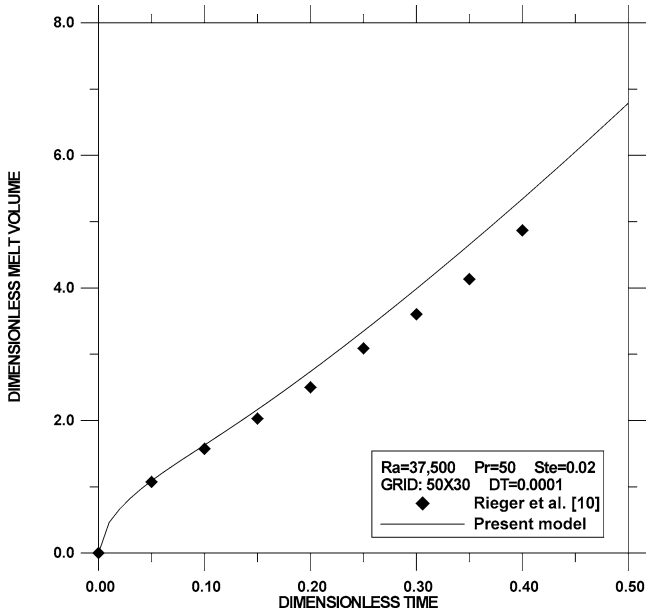

Fig. 9. Comparison of the predicted dimensionless melt volume with the results of Rieger et al. [10] for $Ra = 37\,500$.

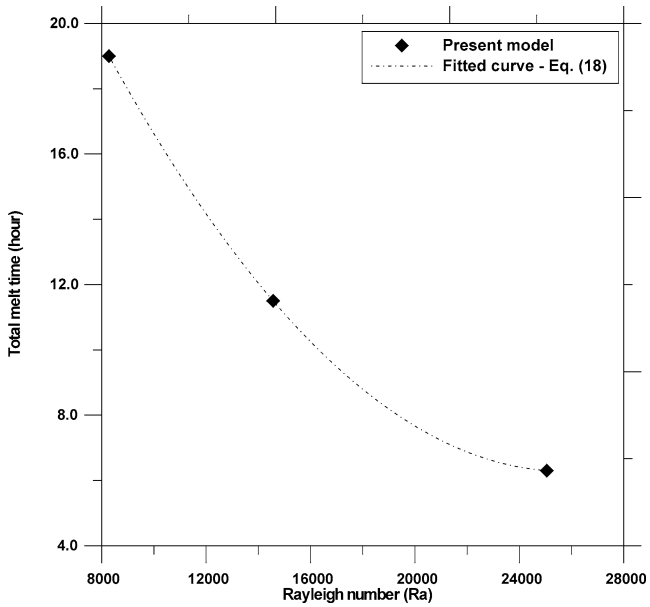

Fig. 10. Total melt time in terms of the Rayleigh number.

means intensification of natural convection and hence major stabilisation of the fusion rate. The effect of Stefan number based on the temperature is similar to the Rayleigh number increase as can be seen in Fig. 11. The correlations relating the time for complete fusion to Rayleigh and Stefan numbers are presented below for the Rayleigh number and Stefan number in the ranges $8281 \leqslant Ra \leqslant 25\,050$ and $0.036 \leqslant Ste \leqslant 0.109$ and for surface temperature of the cylinder, T_o, of 305 to 313 K.

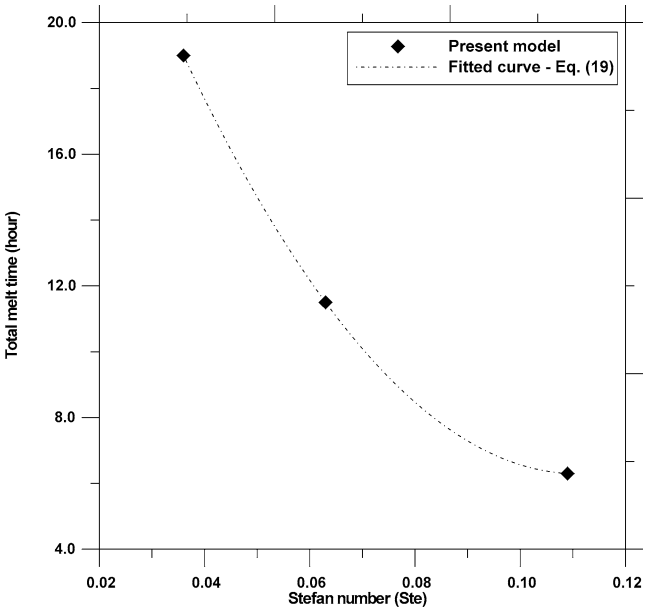

Fig. 11. Total melt time in terms of the Stefan number.

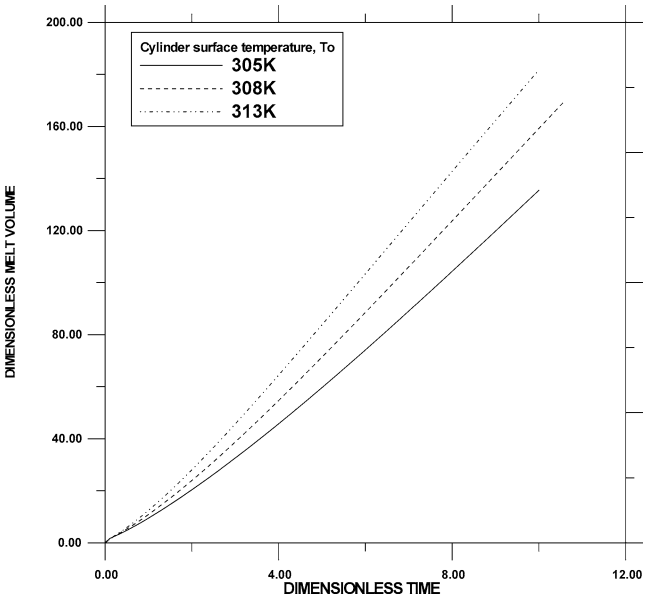

Fig. 12. Total melt volume in terms of the cylinder surface temperatures of 305, 308 and 313 K.

$$\tau_{\text{tot}} = 4.153 \times 10^{-8}(Ra)^2 - 2.142 \times 10^{-3}(Ra) + 33.886 \text{ [hours]} \quad (18)$$

$$\tau_{\text{tot}} = 2256.63(Ste)^2 - 501.184(Ste) + 34.118 \text{ [hours]} \quad (19)$$

The variables shown in the Figs. 10 and 11 as well as in the Figs. 13, 14 and 15 are expressed in dimensional form in order to facilitate the use of the results.

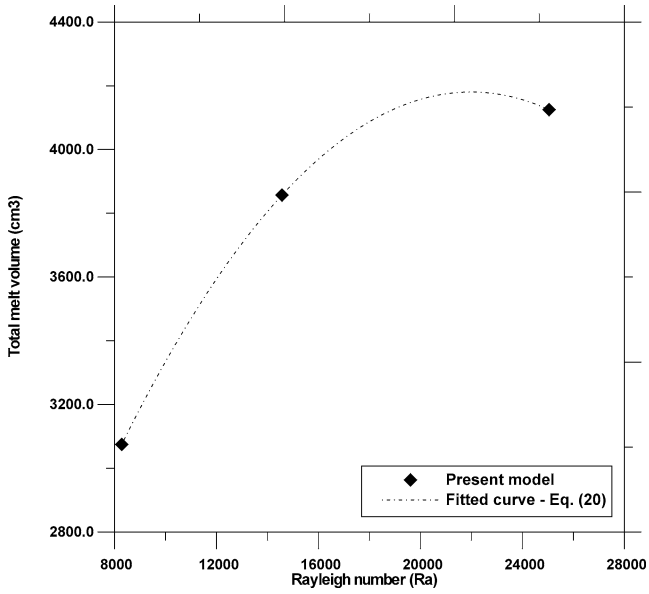

Fig. 13. Total melt volume in terms of the Rayleigh number.

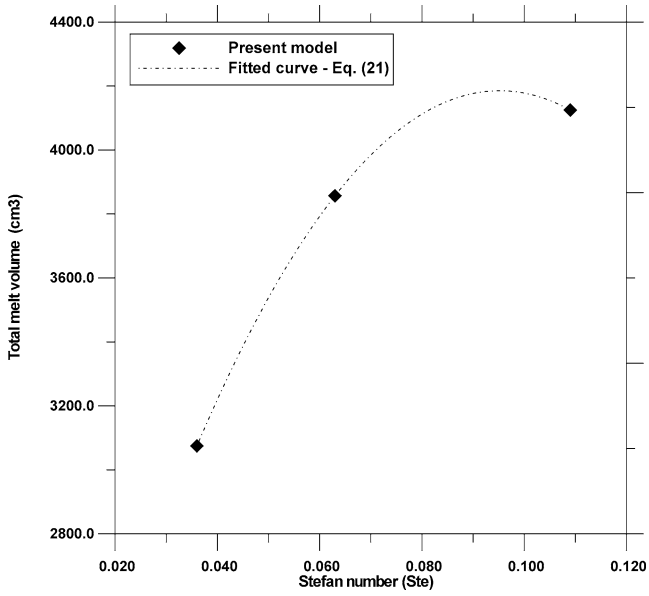

Fig. 14. Total melt volume in terms of the Stefan number.

Fig. 12 shows the total melt volume in terms of three wall temperature of 305, 308 and 313 K. The melt volume is calculated through the expression

$$\forall = \int_0^1 \int_0^\pi R \, \mathrm{d}\theta \, \Delta_L \, \mathrm{d}\eta$$

The present study is two-dimensional and hence the melt volume calculated is considered as being for a unit length.

As is expected the increase of the cylinder wall temperature leads to increase the total melt volume.

Figs. 13–15 shows the effect of the Rayleigh number, Stefan number and the cylinder wall temperature on the total melt volume. As can be seen the increase of Rayleigh

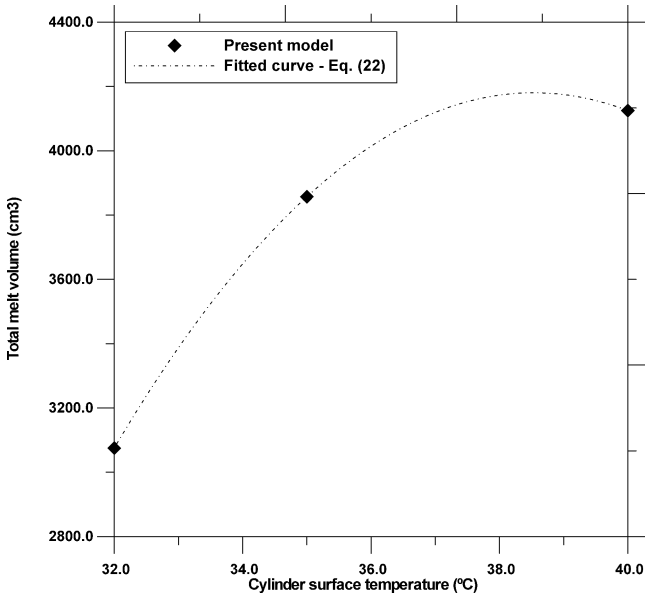

Fig. 15. Total melt volume in terms of the surface temperature of the cylinder.

number leads to increasing the total melt volume rate until about $Ra = 24\,000$. After which the rate of melt volume seems to reach almost steady conditions as explained before. Similar effects are found for the increase of Stefan number based upon the temperature as well as the increase in the cylinder wall temperature. The corresponding correlations for the total melt volume in terms of the Rayleigh number, Stefan number and cylinder wall temperature are presented below

$$\forall_{\text{tot}} = -5.890 \times 10^{-10}(Ra)^2 + 0.259 \times 10^{-4}(Ra) + 1334.64 \times 10^{-4}\ [\text{m}^3{\cdot}\text{m}^{-1}] \quad (20)$$

$$\forall_{\text{tot}} = -316944 \times 10^{-4}(Ste)^2 + 60340.4 \times 10^{-4}(Ste) + 1313.5 \times 10^{-4}\ [\text{m}^3{\cdot}\text{m}^{-1}] \quad (21)$$

$$\forall_{\text{tot}} = -25.883 \times 10^{-4}(T_o)^2 + 1994.85 \times 10^{-4}(T_o) - 34255.7 \times 10^{-4}\ [\text{m}^3{\cdot}\text{m}^{-1}] \quad (22)$$

4. Conclusions

A model is proposed in terms of the primitive variables for the fusion around horizontal circular cylinder including natural convection in the melt region. The phase change front was immobilised by using a coordinate transformation and the method of control volumes was used. The predicted numerical results are compared with available numerical results of Rieger et al. [10]. The agreement is found to be satisfactory indicating that the proposed model is adequate to represent the physical situation of fusion around a horizontal cylinder in the presence of natural convection in the melt region. Additional numerical data and the respective correlations of the effects of Rayleigh number, Stefan number and the cylinder wall temperature on the time for complete phase change and the total melt volume are presented and discussed.

Acknowledgements

The authors wish to thank the CAPES for the scholarships and FAPESP for the financial support.

References

[1] H.G. Landau, Heat conduction in a melting solid, Quart. Appl. Math. 8 (1950) 81–94.
[2] J.L. Duda, M.F. Malone, R.H. Notter, J.S. Ventras, Analysis of two-dimensional diffusion-controlled moving boundary problems, Internat. J. Heat Mass Transfer 18 (1975) 901–910.
[3] T. Saitoh, Numerical method for multi-dimensional freezing problems in arbitrary domains, ASME J. Heat Transfer 100 (1978) 294–299.
[4] E.M. Sparrow, S. Ramadhyani, S.V. Patankar, Effect of subcooling on cylindrical melting, ASME J. Heat Transfer 100 (1978) 395–402.
[5] R.M. Furzerland, A comparative study of numerical methods for moving boundary problems, J. Inst. Math. Appl. 26 (1980) 411–429.
[6] R. Viswanath, Y. Jaluria, A comparison of different solution methodologies for melting and solidification problems in enclosures, Numer. Heat Transfer – Part B 24 (1993) 77–105.
[7] E.M. Sparrow, S.V. Patankar, S. Ramadhyani, Analysis of melting in the presence of natural convection in the melt region, ASME J. Heat Transfer 99 (1977) 520–526.
[8] L.S. Yao, F.F. Chen, Effects of natural convection in the melted region around a heated horizontal cylinder, ASME J. Heat Transfer 102 (1980) 667–672.
[9] L.S. Yao, W. Cherney, Transient phase-change around a horizontal cylinder, Internat. J. Heat Mass Transfer 24 (1981) 1971–1981.
[10] H. Rieger, U. Projahn, H. Beer, Analysis of the heat transport mechanisms during melting around a horizontal circular cylinder, Internat. J. Heat Mass Transfer 25 (1982) 137–147.
[11] J. Prusa, L.S. Yao, Melting around a horizontal heated cylinder: Part I – Perturbation and numerical solutions for constant heat flux boundary condition, ASME J. Heat Transfer 106 (1984) 376–384.
[12] J. Prusa, L.S. Yao, Melting around a horizontal heated cylinder: Part II – Numerical solution for isothermal boundary condition, ASME J. Heat Transfer 106 (1984) 469–472.
[13] J. Herrmann, W. Leindenfrost, R. Viskanta, Melting of ice around a horizontal isothermal cylindrical heat source, Chem. Engrg. Commun. 25 (1984) 63–78.
[14] C.-J. Ho, S. Chen, Numerical simulation of melting of ice around a horizontal cylinder, Internat. J. Heat Mass Transfer 29 (1986) 1359–1369.
[15] E.M. Sparrow, R.R. Schmidt, J.W. Ramsey, Experiments on the role of natural convection in the melting of solids, ASME J. Heat Transfer 100 (1978) 11–16.
[16] N.W. Hale, R. Viskanta, Solid–liquid phase-change heat transfer and interface motion in materials cooled or heated from above or below, Internat. J. Heat Mass Transfer 23 (1980) 283–291.
[17] C. Benard, D. Gobin, A. Zanoli, Moving boundary problem: heat conduction in the solid phase of a phase-change material during melting driven by natural convection in the liquid, Internat. J. Heat Mass Transfer 29 (1986) 1669–1681.